HHS Public Access

Author manuscript

Chem. Author manuscript; available in PMC 2020 September 12.

Published in final edited form as:

Chem. 2019 September 12; 5(9): 2442–2449. doi:10.1016/j.chempr.2019.06.020.

Enzyme-Instructed Peptide Assemblies Selectively Inhibit Bone Tumors

Zhaoqianqi Feng[1,3], **Xiuguo Han**[2,3], **Huaimin Wang**[1], **Tingting Tang**[2,*], **Bing Xu**[1,4,*]

[1]Department of Chemistry, Brandeis University, 415 South Street, Waltham, Massachusetts 02454, United States.

[2]Shanghai Key Laboratory of Orthopaedic Implants, Department of Orthopaedic Surgery, Shanghai Ninth People's Hospital, Shanghai Jiao Tong University School of Medicine, Shanghai, 200011, China.

[3]These authors contributed equally to this work

[4]Lead Contact

SUMMARY

Alkaline phosphatases (ALP) contribute to immunosuppression in solid tumors, but they, unfortunately, are "undruggable". Here we report enzyme-instructed assembly of peptides for selectively inhibiting the tumors that overexpress ALP. We developed a precursor with two parts; an amphiphilic, self-assembling peptides joined to a hydrophilic block (i.e., tyrosine phosphate). ALP, overexpressed on and in osteosarcoma cancer cells (e.g., Saos-2), cleaves the phosphates from the tyrosine residue of the precursor and triggers the self-assembly of the resulting peptides. Being selectively formed on and inside the cancer cells, the peptide assemblies induce the cancer cell death and efficiently inhibit the tumor growth in an orthotopic osteosarcoma mice model without harming normal organs. Accordingly, the peptide assemblies significantly improve the survival ratio of metastatic tumor bearing mice. Without relying on inhibiting ALP, this approach integrates enzyme reaction and molecular self-assembly for generating peptide fibrils as potential anticancer therapeutics.

INTRODUCTION

Despite the significant advances cancer immunotherapy based on checkpoint blockade,[1] immunosuppressive adenosine[2] in tumor microenvironment is a major cause for the patients' unresponsiveness to the treatment.[3] Among the mechanisms for generating extracellular

*Correspondence: ttt@sjtu.edu.cn, bxu@brandeis.edu.

AUTHOR CONTRIBUTIONS

B. X. and Z.F. conceived the study. Z.F. designed and performed the chemical synthesis, cell free and cell based assays, analyzed the experimental results. H.W. synthesized some compounds. X.H. performed in vivo experiments with input from Z.F.. T.T. gave professional suggestions on the in vivo experiments. B.X. supervised the studies. B. X. and Z.F. wrote the manuscript with the input from all authors.

SUPPLEMENTAL INFORMATION

Supplemental Information includes 12 Figures, 1 Video, Experimental Procedures, Synthesis and characterization of the compounds.

COMPETING FINANCIAL INTERESTS

The authors declare no competing financial interests

adenosine to suppress anticancer immunity, alkaline phosphatase (ALP)[4–6], as an enzymes overexpressed at stem cells[7] and certain cancer cells,[8] rapidly converts ATP to adenosine (Fig. 1). A conventional strategy to address this problem would be inhibiting ALP activity. ALP, however, is regarded as “undruggable”, though it was identified as a cancer marker over half-century ago.[9, 10] It remains a challenge for developing suitable inhibitors[11] for ALP without causing harmful side effects because ALP ubiquitously presents in all tissues (especially at liver, bone, intestine, and placenta) and plays a critical role in embryogenesis, bone metabolism, and neuron functions.[11, 12] Thus, it would be beneficial to develop an out-of-box approach that kills the ALP-overexpressing cancer cells selectively without relying on ALP inhibition.

Enzyme-instructed assembly[13] of peptides turns out to be effective for killing ALP-overexpressing cancer cells.[14–17] Bypassing the need of inhibiting ALP, this approach integrates ALP-catalyzed dephosphorylation and self-assembly for generating the fibrils of small molecules (e.g., ultrashort peptides, hexoses, or cholesterols) as the anticancer therapeutics. For example, a precursor has two parts; an amphiphilic, self-assembling peptides joined to a tyrosine phosphate, which renders the precursor water soluble. ALP overexpressed on cancer cells cleaves the phosphate and triggers the self-assembly of the peptides. Being selectively formed on and inside the cancer cells (Fig. 1), the peptides assemblies induce the cancer cell death by activating extrinsic cell death receptors[18] and/or generating intracellular cell stresses.[14, 17, 19] Besides being applied for imaging the activity of ALP on cell surface,[20] this approach has been applied to selectively kill undifferentiated iPS cells in a cell mixture without harming the muscle cells that are differentiated from the iPS cells for a successful transplantation in a murine model.[21]

Despite the demonstration of ALP-instructed peptide assemblies for selectively inhibiting cancer cells in cell assays, there is, however, a major obstacle for applying this approach in vivo, which is the liver toxicity because the ALP expressed in liver tissue[22] would also generate the peptide assemblies. Recently, we have overcome this drawback by developing a precursor that is the substrate of ALP as well as that of carboxylesterase (CES). Being expressed in mammalian liver tissue,[23, 24] CES accelerates the disassembly of the peptide assemblies for detoxifying in liver cells.[25] This advance confers excellent selectivity to the precursor for killing cancer cells over hepatocytes,[25] thus allowing in vivo evaluation of the antitumor efficacy of ALP-instructed assembly of peptides.

To investigate in vivo tumor inhibition by ALP-instructed assembly of peptides, we chose an orthotopic murine model of human metastatic osteosarcoma.[26] Metastatic osteosarcoma expresses relatively low level of PD-L1[27], but very high level of ALP,[28] which leads to little improvement in patient survival and regression of osteosarcoma lung metastasis after immunotherapy.[27] In addition, the ALP overexpression in osteosarcoma warrants fast dephosphorylation for selective tumor targeting and high anticancer efficacy. We evaluated the precursors using the murine model. Our results validate that ALP instructs the assembly of peptides for effectively inhibiting osteosarcoma tumor in vivo. Specifically, ALP catalytically dephosphorylates the precursors to generate the assemblies of the peptides. Such a multistep molecular process[15] efficiently inhibits the tumor growth in an orthotopic osteosarcoma mice model without damaging normal tissues, and significantly improve the

survival ratio of metastatic tumor bearing mice. Validating the in vivo anticancer efficacy of enzyme-instructed assembly of peptides for the first time, this work illustrates a fundamentally new way based on kinetics (i.e., enzymatic peptide assembling process) for targeting immunosuppressive cancer cells, and it contributes to use supramolecular for establishing immune normalization in cancer treatment.

RESULTS AND DISCUSSION

Molecular design and self-assembly

The ALP-instructed assembly, involving Nap-ffy$_p$e$_{Me2}$ (**1P**) and Nap-ffye$_{Me2}$ (**1**) (Fig. 1), selectively and effectively inhibits an osteosarcoma *in vitro*. We used lower case one-letter codes to refer to D-amino acids here. Consisting of a self-assembling peptide backbone (2-(naphthalen-2-yl)acetyl)-D-phenylalanyl-D-phenylalanine (Nap-ff)), a dephosphorylation site (D-phosphotyrosine (y$_p$)), and an esterase detoxification substrate (dimethyl-D-glutamate (e$_{Me2}$)), Nap-ffy$_p$e$_{Me2}$ self-assembles to form nanoparticles and/or nanofibrils, depending on its concentrations.[29] For example, at 200 μM, it forms a mixture of amorphous solid and scanted numbers of nanofibers. Upon ALP-catalyzed dephosphorylation, the Nap-ffy$_p$e$_{Me2}$ becomes Nap-ffye$_{Me2}$, which forms a network of uniform nanofibers with a diameter of 12 ± 2 nm (Fig. 2A). Such a molecular process is rather general because ALP-instructed assembly of analogs of **1P**/**1** also results in similar morphology transition.[29]

ALP-instructed assembly in live cells

Saos-2, an osteosarcoma cell line, overexpresses ALP to convert Nap-ffy$_p$e$_{Me2}$ into Nap-ffye$_{Me2}$, instructing the assemblies of Nap-ffye$_{Me2}$ on and inside Saos-2 cells to result in cell death within half an hour (Fig. 2B). While Nap-ffy$_p$e$_{Me2}$ potently inhibits Saos-2 cells (IC$_{50}$ = 4 μM), its IC$_{50}$ on the hepatocyte cells (HepG2) is over two orders of magnitude higher than the IC$_{50}$ on Saos-2 (Figure 2C). This result is particular important because it indicates that Nap-ffy$_p$e$_{Me2}$ can selectively inhibit the osteosarcoma cells without harming liver cells.

To directly visualize the cellular distribution of the ALP-instructed peptide assemblies, we employed NBD-ffy$_p$e$_{Me2}$ (**F1P**), a fluorescent analogue of Nap-ffy$_p$e$_{Me2}$. (Fig 2D) We chose environment sensitive fluorescent probe NBD because it exhibits enhanced fluorescence upon the formation of supramolecular assemblies.[20] Incubating NBD-ffy$_p$e$_{Me2}$ with Saos-2 cells for 0.5 h results in bright fluorescence in the cytoplasm of Saos-2, together with a few fluorescent puncta on the cell membrane (Fig. 2E and Video S1). This observation confirms that ALPs, on and inside the Saos-2 cells, instruct the assembly of the peptides on the surface and in the cytosol of the cells. Replacing the dimethyl-D-glutamate (e$_{Me2}$) in NBD-ffy$_p$e$_{Me2}$ with glutamate generates NBD-ffy$_p$e (**F4P**). Incubating Saos-2 with NBD-ffy$_p$e only generates several intracellular fluorescent puncta. These results suggest that the methylation of glutamate significantly enhances the uptake of the precursors by the Saos-2 cells.

ALP-instructed assembly inhibits tumor growth

Nap-ffy$_p$e$_{Me2}$ potently inhibits Saos2-luc and Saos2-lung cells,[26] with an IC$_{50}$ value of 8.4 and 3.2 μM, respectively (Fig. 3A). This result agrees with the slightly lower expression

level of ALP on Saso2-luc compared with Saos2-lung cells (Fig. 3B). To establish the orthotopic mouse model of osteosarcoma, we injected luciferase-labeled Saos-2 cells (Saos2-luc) and its highly metastatic subtype (Saos2-lung) cells into the bone marrow cavity of the mouse tibia and started the treatment until tumors had reached 100 mm^3 in size.[30] After treating the tumor bearing mice with the Nap-ffy_pe_{Me2} and saline for four weeks, the mice were sacrificed and the tumor volumes were measured. Treating with Nap-ffy_pe_{Me2} results in the 8-fold and 25-fold reduction in tumor volume of Saos2-luc and Saos2-lung, respectively (Fig. 3C, D, S4), indicating that the Nap-ffy_pe_{Me2} effectively inhibits the tumor. To monitor the tumor growth in real-time, bioluminescence of tumor cells was measured at 1, 2, 3 and 4 weeks after the treatment (Fig. 3E). The results further confirms that Nap-ffy_pe_{Me2} efficiently inhibit the tumor growth of osteosarcoma (Fig. 3F), and exhibit higher efficacy against the metastatic osteosarcoma (Saos2-lung). Moreover, the treatment significantly prolongs the survival time of the osteosarcoma-bearing nude mice (Fig. 3G), confirming the benefits of Nap-ffy_pe_{Me2} treatment.

Evaluation of selectivity and systemic toxicity

After treating with Nap-ffy_pe_{Me2} or saline for 4 weeks, the mice were sacrificed and the tumor were dissected and stained with haematoxylin and eosin (HE) (Fig. 4A). Compared with the saline group, majority of the cells in the Nap-ffy_pe_{Me2} treatment group exhibit nuclear condensation, as well as scattering broken nuclei, indicating that Nap-ffy_pe_{Me2} induced tumor apoptosis *in vivo*. To further validate the tumor apoptosis, we conducted the terminal deoxynucleotidyl transferase dUTP nick end labeling (TUNEL) assay. Treating with Nap-ffy_pe_{Me2}, most of cells in tumor tissue exhibit brown (TUNEL positive) indicative for DNA fragmentation (Fig. 4B), resulting in the 7-fold and 11-fold increase in TUNEL signals of Saos2-luc and Saos2-lung, respectively (Fig. 4C). To evaluate the systemic toxicity of Nap-ffy_pe_{Me2}, major organs (heart, liver, spleen, kidney, and lung) were prepared for histological analysis after the treatment. As shown in Fig. 4D and Fig. S6, no observable difference was noticed between the Nap-ffy_pe_{Me2} treatment group and saline group, indicating excellent biocompatibility of the peptide assemblies.

Structural Analogs for target validation

To validate the target (ALP) through molecular design,[31] we synthesized another two ALP cleavage precursors Nap-$ffy_p{}^hR$ (**2P**)[32] and Npx-$ffy_p{}^hR$ (**3P**, Npx is naproxen)[33] and evaluated their anticancer activities *in vitro* and *in vivo*. The *in vitro* assay reveals that the anticancer efficacy of the precursors against osteosarcoma cells follows the order of **1P** > **2P** > **3P** (Figs. S7 and S8). Compared with **1P**, **2P** and **3P** exhibit reduced selectivity for targeting osteosarcoma cells over hepatocyte cells (Fig. S8), agreeing with that the esterases in liver cells are unable to act on them. These results address the importance of ester bonds in the molecule design of **1P**, which not only increases the efficacy of **1P**, but also enables the dissociation of assemblies by esterase in hepatocyte cells to result in minimized cytotoxicity to hepatocyte cells. Although **2P** and **3P** also inhibit the tumor growth in the orthotopic mouse model of osteosarcoma, their inhibitory efficacies follow the same trend of the *in vitro* assay (Figs. S9 and 10). These results, nevertheless, indicate that integrating the molecular design of small molecule for instructed-assembly with bioinformatics (e.g.,

overexpression of CES in liver[34]) opens a new window for precision medicine and minimizing the side effect.

Conclusion

In conclusion, this work demonstrates enzyme-instructed supramolecular assemblies of peptides to target immunosuppressive tumors *in vivo*. Although this work used osteosarcoma, the principle demonstrated here should be applicable to any other ALP expressing tumors, like high-grade serous ovarian cancer OVSAHO.[25] Since aggregation of small molecules is a general phenomenon[35], this work, which relies on assemblies of small molecules, may lead a way to resurrect drug candidates discarded due to aggregations because the formation of in-situ assemblies in tumor could reduce the diffusion and enhance the tumor retention. Moreover, a major obstacle in anticancer nanomedicine is liver accumulation, which currently is circumvented by using cells to carry the nanoparticles.[36] The approach in this work allows precursors to be soluble monomers before they reach tumor and form nanofibrils in-situ at the tumor, thus would minimize the liver accumulation.

EXPERIMENTAL PROCEDURES

Full experimental procedures are provided in the Supplemental Information.

Supplementary Material

Refer to Web version on PubMed Central for supplementary material.

ACKNOWLEDGEMENTS

This work was partially supported by NIH (CA142746) to B. X., NSF (DMR-1420382) to B. X. and NIH (F99CA234746) to Z.F. We also want to thank National key R&D program of China (2016YFC1102100) to T. T., National Natural Science Foundation of China (81672205) to T. T. and Innovation Program for PhD students in Shanghai Jiao Tong University School of Medicine (BXJ201829) to X.H.

REFERENCES

1. Sanmamed MF, Chen L. (2018). A Paradigm Shift in Cancer Immunotherapy: From Enhancement to Normalization. Cell 175, 313–326. [PubMed: 30290139]
2. Di Virgilio F, Sarti AC, Falzoni S, De Marchi E, Adinolfi E. (2018). Extracellular ATP and P2 purinergic signalling in the tumour microenvironment. Nat. Rev. Cancer 18, 601–618. [PubMed: 30006588]
3. Vijayan D, Young A, Teng MWL, Smyth MJ. (2017). Targeting immunosuppressive adenosine in cancer. Nat. Rev. Cancer 17, 709–724. [PubMed: 29059149]
4. Rao SR, Snaith AE, Marino D, Cheng X, Lwin ST, Orriss IR, Hamdy FC, Edwards CM. (2017). Tumour-derived alkaline phosphatase regulates tumour growth, epithelial plasticity and disease-free survival in metastatic prostate cancer. Br. J. Cancer 116, 227–236. [PubMed: 28006818]
5. Pettengill M et al. (2013). Soluble Ecto-5 ‘-nucleotidase (5 ‘-NT), Alkaline Phosphatase, and Adenosine Deaminase (ADA1) Activities in Neonatal Blood Favor Elevated Extracellular Adenosine. J. Biol. Chem 288, 27315–27326. [PubMed: 23897810]
6. Kim SH, Shin K-H, Moon S-H, Jang J, Kim HS, Suh J-S, Yang W-I. (2017). Reassessment of alkaline phosphatase as serum tumor marker with high specificity in osteosarcoma. Cancer Med. 6, 1311–1322. [PubMed: 28493412]

7. Shamblott MJ, Axelman J, Wang SP, Bugg EM, Littlefield JW, Donovan PJ, Blumenthal PD, Huggins GR, Gearhart JD. (1998). Derivation of pluripotent stem cells horn cultured human primordial germ cells. Proc. Natl. Acad. Sci. U. S. A 95, 13726–13731. [PubMed: 9811868]
8. Fishman WH. (1987). Clinical and biological significance of an isozyme tumor marker--PLAP. Clin. Biochem 20, 387–392. [PubMed: 3325192]
9. Bernhard A, Rosenbloom L. (1953). Ion exchange effect on alkaline phosphatase of serum with reference to cancer. Science 118, 114–115. [PubMed: 13076207]
10. Fishman WH, Inglis NR, Green S, Anstiss CL, Gosh NK, Reif AE, Rustigia R, Krant MJ, Stolbach LL. (1968). Immunology and biochemistry of Regan isoenzyme of alkaline phosphatase in human cancer. Nature 219, 697–699. [PubMed: 5691166]
11. Millán JL, Mammalian Alkaline Phosphatases: From Biology to Applications in Mdicine and Biotechnology. (John Wiley & Sons, 2006).
12. Fonta C, Négyessy L, Neuronal Tissue-Nonspecific Alkaline Phosphatase (TNAP) Subcellular Biochemistry (Springer, 2015).
13. He HJ, Xu B. (2018). Instructed-Assembly (iA): A Molecular Process for Controlling Cell Fate. Bull. Chem. Soc. Jpn 91, 900–906. [PubMed: 30559507]
14. Wang HM, Feng ZQQ, Wang YZ, Zhou R, Yang ZM, Xu B. (2016). Integrating Enzymatic Self-Assembly and Mitochondria Targeting for Selectively Killing Cancer Cells without Acquired Drug Resistance. J. Am. Chem. Soc 138, 16046–16055. [PubMed: 27960313]
15. Zhou J, Du XW, Yamagata N, Xu B. (2016). Enzyme-Instructed Self-Assembly of Small D-Peptides as a Multiple-Step Process for Selectively Killing Cancer Cells. J. Am. Chem. Soc 138, 3813–3823. [PubMed: 26966844]
16. Pires RA, Abul-Haija YM, Costa DS, Novoa-Carballal R, Reis RL, Ulijn RV, Pashkuleva I. (2015). Controlling Cancer Cell Fate Using Localized Biocatalytic Self-Assembly of an Aromatic Carbohydrate Amphiphile. J. Am. Chem. Soc 137, 576–579. [PubMed: 25539667]
17. Wang HM, Feng ZQQ, Wu DD, Fritzsching KJ, Rigney M, Zhou J, Jiang YJ, Schmidt-Rohr K, Xu B. (2016). Enzyme-Regulated Supramolecular Assemblies of Cholesterol Conjugates against Drug-Resistant Ovarian Cancer Cells. J. Am. Chem. Soc 138, 10758–10761. [PubMed: 27529637]
18. Du XW, Zhou J, Wang HN, Shi JF, Kuang Y, Zeng W, Yang ZM, Xu B. (2017). In situ generated D-peptidic nanofibrils as multifaceted apoptotic inducers to target cancer cells. Cell Death Dis. 8,
19. Feng Z, Wang H, Wang S, Zhang Q, Zhang X, Rodal AA, Xu B. (2018). Enzymatic Assemblies Disrupt the Membrane and Target Endoplasmic Reticulum for Selective Cancer Cell Death. J. Am. Chem. Soc 140, 9566–9573. [PubMed: 29995402]
20. Zhou J, Du XW, Berciu C, He HJ, Shi JF, Nicastro D, Xu B. (2016). Enzyme-Instructed Self-Assembly for Spatiotemporal Profiling of the Activities of Alkaline Phosphatases on Live Cells. Chem 1, 246–263. [PubMed: 28393126]
21. Kuang Y et al. (2017). Efficient, selective removal of human pluripotent stem cells via ecto-alkaline phosphatase-mediated aggregation of synthetic peptides. Cell Chem. Biol 24, 685–694. e684. [PubMed: 28529132]
22. Kaplan MM. (1972). Alkaline Phosphatase. N. Engl. J. Med 286, 200–202. [PubMed: 4550137]
23. Ross MK, Borazjani A, Wang R, Crow JA, Xie SQ. (2012). Examination of the carboxylesterase phenotype in human liver. Arch. Biochem. Biophys 522, 44–56. [PubMed: 22525521]
24. Satoh T, Hosokawa M. (1998). The mammalian carboxylesterases: From molecules to functions. Annu. Rev. Pharmacol. Toxicol 38, 257–288. [PubMed: 9597156]
25. Feng Z, Wang H, Zhou R, Li J, Xu B. (2017). Enzyme-Instructed Assembly and Disassembly Processes for Targeting Downregulation in Cancer Cells. J. Am. Chem. Soc 139, 3950–3953. [PubMed: 28257192]
26. Du L, Fan QM, Tu B, Yan W, Tang TT. (2014). Establishment and characterization of a new highly metastatic human osteosarcoma cell line derived from Saos2. Int. J. Clin. Exp. Pathol 7, 2871–2882. [PubMed: 25031706]
27. Dhupkar P, Gordon N, Stewart J, Kleinerman ES. (2018). Anti-PD-1 therapy redirects macrophages from an M2 to an M1 phenotype inducing regression of OS lung metastases. Cancer Med. 7, 2654–2664. [PubMed: 29733528]

28. Rodan SB, Imai Y, Thiede MA, Wesolowski G, Thompson D, Barshavit Z, Shull S, Mann K, Rodan GA. (1987). Characterization of a human osteosarcoma cell line (Saos-2) with osteoblastic properties. Cancer Res. 47, 4961–4966. [PubMed: 3040234]

29. Feng Z, Wang H, Chen X, Xu B. (2017). Self-Assembling Ability Determines the Activity of Enzyme-Instructed Self-Assembly for Inhibiting Cancer Cells. J. Am. Chem. Soc 139, 15377–15384. [PubMed: 28990765]

30. Han XG, Du L, Qiao H, Tu B, Wang YG, Qin A, Dai KR, Fan QM, Tang TT. (2015). CXCR1 knockdown improves the sensitivity of osteosarcoma to cisplatin. Cancer Lett. 369, 405–415. [PubMed: 26391645]

31. Sweis RF. (2015). Target (In)Validation: A Critical, Sometimes Unheralded, Role of Modern Medicinal Chemistry. ACS Med. Chem. Lett 6, 618–621. [PubMed: 26101559]

32. Feng ZQQ, Wang HM, Wang SY, Zhang Q, Zhang XX, Rodal AA, Xu B. (2018). Enzymatic Assemblies Disrupt the Membrane and Target Endoplasmic Reticulum for Selective Cancer Cell Death. J. Am. Chem. Soc 140, 9566–9573. [PubMed: 29995402]

33. Feng Z, Wang H, Xu B. (2018). Instructed Assembly of Peptides for Intracellular Enzyme Sequestration. J. Am. Chem. Soc 140, 16433–16437. [PubMed: 30452246]

34. Uhlen M et al. (2015). Tissue-based map of the human proteome. Science 347,

35. Irwin JJ, Duan D, Torosyan H, Doak AK, Ziebart KT, Sterling T, Tumanian G, Shoichet BK. (2015). An Aggregation Advisor for Ligand Discovery. J. Med. Chem 58, 7076–7087. [PubMed: 26295373]

36. Tang L et al. (2018). Enhancing T cell therapy through TCR-signaling-responsive nanoparticle drug delivery. Nat. Biotechnol 36, 707–716. [PubMed: 29985479]

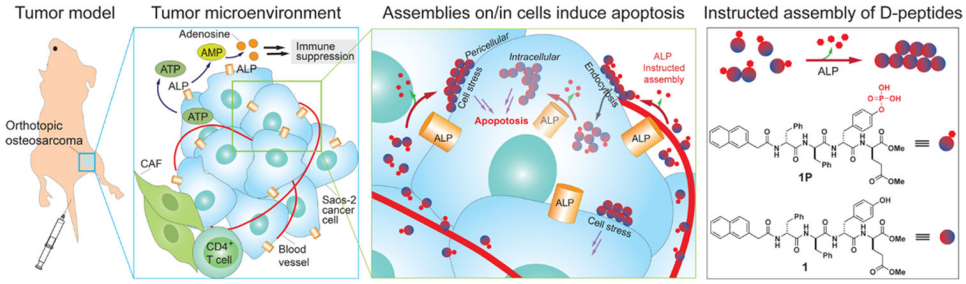

Figure 1.

Schematic representation of ALP-instructed assembly for inhibiting metastatic osteosarcoma within an immunosuppressive tumor microenvironment in an orthotopic mice model and molecular structures of the precursor (**1P**) and hydrogelator (**1**).

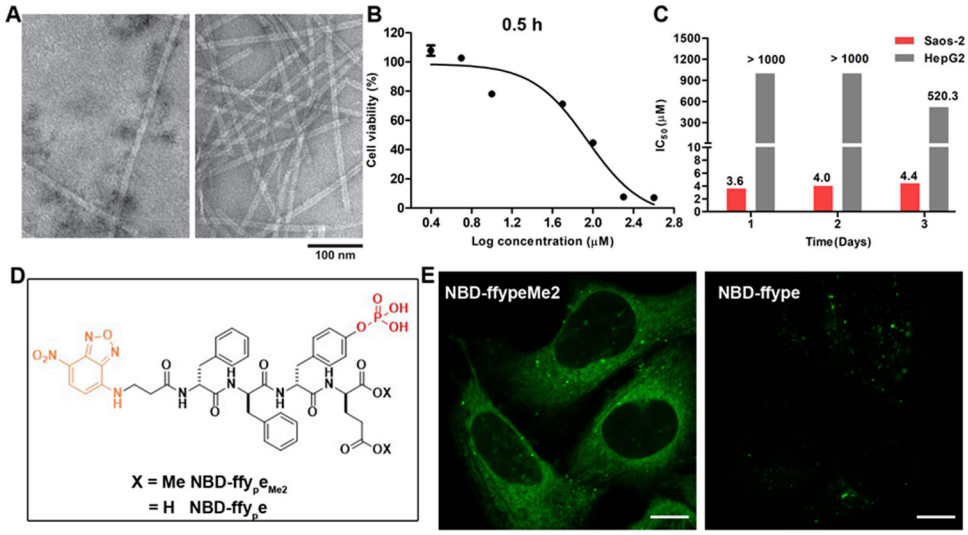

Figure 2.

ALP-instructed assembly of peptides in cell-free conditions and in live cells. (A) Transmission electron microscope (TEM) images of nanostructures formed before and after adding ALP (2 U/mL) to the solution of **1P** (200 μM). (B) Cell viability of Saos-2 cells treated with **1P** for 0.5 h. (C) IC_{50} values of **1P** (24 h, 48 h, 72 h) against Saos-2 or HepG2 cells. (D) Molecular structures of NBD-ffy$_p$e$_{Me2}$ and NBD-ffye. (E) CLSM images of Saos-2 cells treated with NBD-ffy$_p$e$_{Me2}$ or NBD-ffye (200 μM) for 0.5 h. Scale bars, 10 μm.

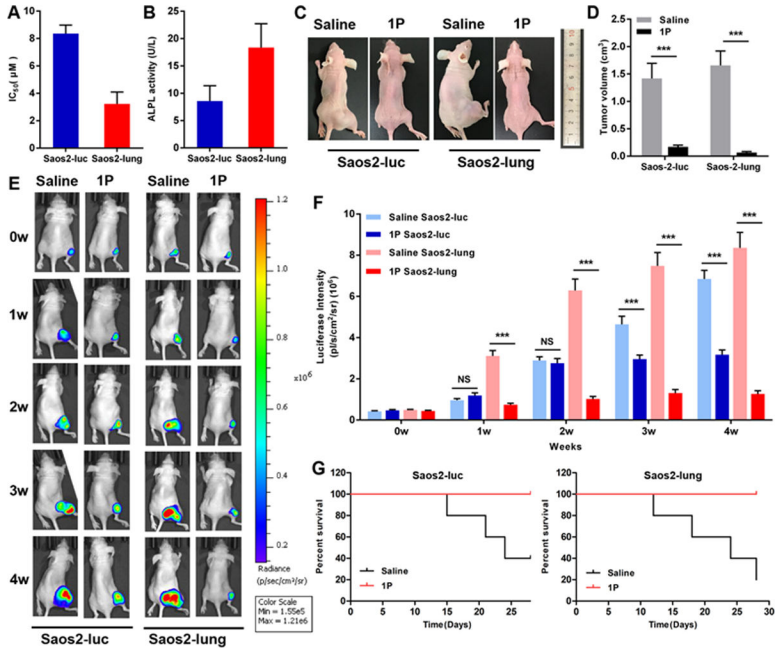

Figure 3.

ALP-instructed assembly of peptides inhibits the tumor growth in an orthotopic osteosarcoma mice model. (A) IC_{50} values of **1P** against Saos2-luc and Saos2-lung cells. (B) ALP activities on Saso2-luc and Saos2-lung cells. (C and D) Tumor volume of orthotopic osteosarcoma model established by Saos2-luc and Saos2-lung cells after tail intravenous injection of compound **1P** or saline for 4 weeks. (E) Images of osteosarcoma tumor growth using in vivo imaging system (IVIS) for orthotopic osteosarcoma model established by Saos2-luc and Saos2-lung cells at week 1–4 after **1P** or saline treatment. (F) Quantification of luciferase intensity. (G) Kaplan-Meier survival curves for orthotopic osteosarcoma nude mice (n = 5) treated with **1P**. Data are presented as mean ± standard deviation (S.D.). NS, not significant, ***$P < 0.001$.

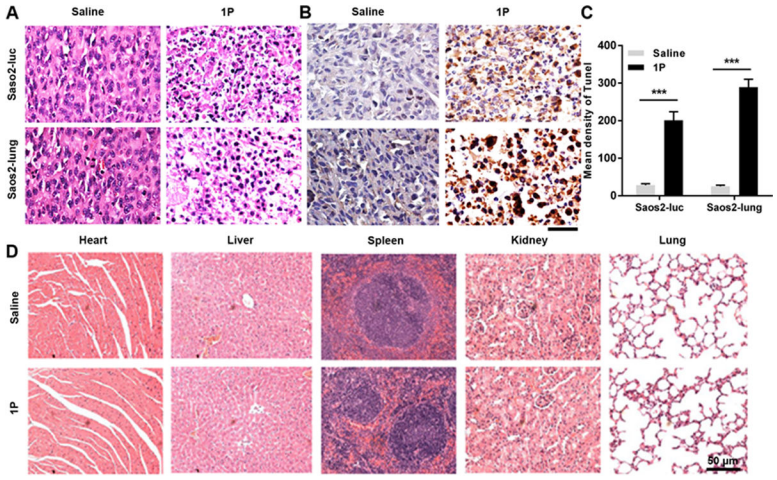

Figure 4.

ALP-instructed assembly of peptides induces tumor apoptosis without harming normal tissues. (A and B) Representative images of (A) HE staining and (B) TUNEL staining of the dissected tumors from nude mice treated with **1P** or saline for 4 weeks. Scale bar, 50 μm. (C) Quantification of TUNEL signals in (B). (D) Images of HE staining of major organs (heart, liver, spleen, kidney, and lung) harvested after treating the osteosarcoma-bearing nude mice, established by Saos2-lung cells, with **1P** or saline for 4 weeks. Scale bar, 50 μm.